ANNALS OF FACULTY ENGINEERING HUNEDOARA
– INTERNATIONAL JOURNAL OF ENGINEERING
Tome X (Year 2012) – FASCICULE 3 (ISSN 1584 – 2673)

[1.]S.Syath ABUTHAKEER, [2.]P.V. MOHANRAM, [3.] G. Mohan KUMAR

DYNAMIC CHARACTERISTICS ANALYSIS OF HIGH SPEED MOTORIZED SPINDLE

[1,2] DEPARTMENT OF MECHANICAL ENGINEERING, PSG COLLEGE OF TECHNOLOGY, COIMBATORE – 641 004, INDIA
[3] PARK COLLEGE OF ENGINEERING AND TECHNOLOGY, COIMBATORE, INDIA

ABSTRACT: *High speed machining (HSM) is a capable technology for drastically increasing productivity and reducing production costs. Development of high-speed spindle technology is strategically critical to the implementation of HSM. Compared to conventional spindles, motorized spindles are equipped with built-in motors for better power transmission and balancing to achieve high-speed operation. However, the built-in motor introduces a great amount of heat into the spindle system as well as additional mass to the spindle shaft, thus complicating its thermo-mechanical- dynamic behaviors. This paper presents a Finite element analysis of dynamic characteristics of high speed motorized spindle using ANSYS. It includes the finite element selection, boundary condition, numerical formulae for finding input parameters to the ANSYS. This analysis is used to extract natural frequencies and mode shapes of the high speed motorized spindle including gyroscopic and centrifugal effects. The dynamic characteristics and modal characteristics of motorized spindles were analyzed experimentally. Numerical analysis was done and results were validated with experimental results.*
KEYWORDS: *High-speed motorized spindle,Natural frequency, Lab VIEW, ANSYS*

INTRODUCTION AND LITERATURE SURVEY

High-speed motorized spindle technology is of great significance to the research and development of high-speed machine tool. The technology of HSM is still relatively new. Although theories of high-speed metal cutting were Reported in the 1930s [1] machine tools capable of Achieving these cutting speeds did not exist commercially until the 1980s [2,3]. Only recently, industry has started experimenting with the use of HSM in production. The aircraft industry was first, with the automotive industry and mold and die maker snow following. Because of the lack of experience in this new field, there are still many problems to be solved in the application of HSM. Current problems include issues of tooling, balancing, thermal and dynamic behaviors, and reliability of machine tools. HSM is often associated with high feed rates which require rapid acceleration and deceleration, resulting in drastic changes in cutting conditions. In the aerospace industry the use of long tools to generate deep pockets puts tremendous stress on the spindle and the cutter. Development of high-speed spindle technology is strategically critical to the implementation of HSM.

To achieve high-speed rotation, motorized spindles have been developed. This type of spindle is equipped with a built-in motor as an integrated part of the spindle shaft, eliminating the need for conventional power trans-mission devices such as gears and belts. This design reduces vibrations, achieves high rotational balance, and enables precise control of rotational accelerations and decelerations. However, the high-speed rotation and the built-in motor also introduce large amounts of heat and rotating mass in to the system, requiring precisely regulated cooling, lubrication, and balancing. As a result, the thermal and mechanical behaviors of high-speed motorized spindles have become very difficult to predict for spindle designers and users. Furthermore, the high-speed rotation also renders many conventional testing techniques unsuccessful at determining spindle behaviors during very high-speed rotation. Only recently, comprehensive thermal characterization of motorized spindles were reported by Bossmanns and Tu [4,5] to quantify heat sources, heat sinks and the heat transfer mechanism of an entire motorized spindle under the influence of speed and bearing preload. This model is capable of predicting the temperature growth of an entire motorized spindle system, including the rotating components, across a wide speed range. This model is verified on a high-speed machining test bed equipped with a custom-built high performance motorized spindle of 32KW and a maximum speed of 25,000 rpm (1.5 million DN). The high speed machining process requests completely new demands for the mechanism of such processing equipment, as due to the process, path speeds exceeding 50m/min can be achieved. In this field, potential capacities of manufacturing processes require a dynamic behavior ten times higher than conventional machine tools and increased accuracy. This can be solved by the systematical evaluation of suitable machine kinematics, by the application of linear direct drives as well as by mass reduction of the axis through light weight components of sheet metal. The requirements of high speed machining and ways to improve the performance of machine tool have been studied [6]. The energy flow model of high-speed motorized spindle further, and

analyzed the quantitative model reflecting the heating value of spindle [7]. The dynamic effects of the spindle using Timoshenko beam theory were studied [8].

In this paper, the FEM model of motorized spindle is set up to research on its modal and dynamic characteristics, which is effected by the axial preload on the natural frequency, the motorized spindle's natural frequencies and corresponding vibration shapes, centrifugal forces and gyroscopic moments on the motorized spindle shaft. The mass distribution of rotor, the non-linearity of bearing rigidity and the whirling motion of spindle are taken into account in modeling.

STRUCTURE OF THE SPINDLE

The spindle parts are supported by two sets of angular contact ceramic ball bearing in front and one set of angular contact ceramic ball bearing in rear which is installed back to back. The motor is set between front second set and rear bearings. As one whole body, the stator and coolant jacket are installed to the shell of spindle. Two lock nuts are used to give preload. One lock nut is positioned at the second set of the front bearing with front preload spacer.

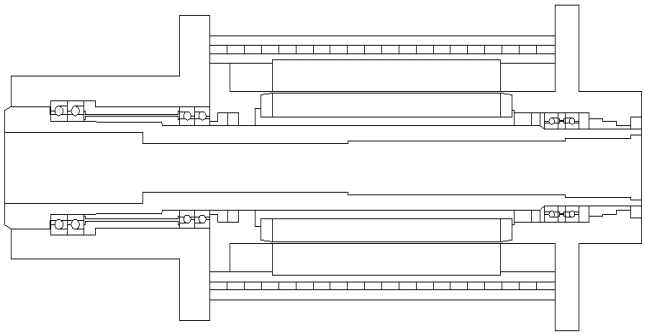

Figure 1. Structure of the high speed spindle

Another one is placed at the rear set of bearings with rear preload spacer. Front and rear bearing housings are placed over the bearing systems. The coolant jacket is placed over the stator-rotor system and outer body is placed over the coolant jacket. The main spindle, front and back bearing systems, stator-rotor system coolant jacket is shown in figure 1 and the outer body are only considered in the high speed motorized spindle in both thermal and vibration analysis. The sensor ring and servo controller of the high speed motorized spindle are not included in both the analysis.

EXPERIMENTAL MODAL ANALYSIS OF HIGH SPEED SPINDLE

The vibration response of the spindle was obtained using impact testing, where an instrumented hammer was used to excite the spindle its free end. The resulting vibration was measured using a low mass accelerometer. The experimental setup consisted of an impact hammer, a charge accelerometer; signal conditioner and data acquisition is shown in figure 2. This experimental setup was used to find the modal characteristics of the spindle.

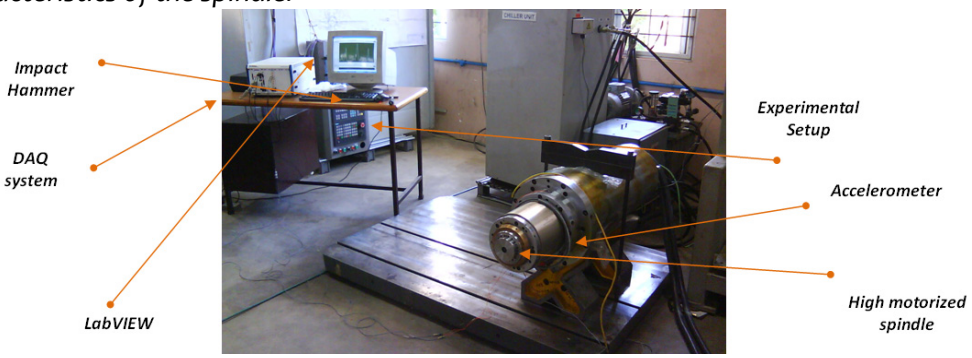

Figure 2. Experimental setup

The program in LabVIEW 8.2 was developed for measuring the response of spindle for excitation given by the hammer using data acquisition system.

The excitation by impact was given to spindle by impact hammer and thus the response was obtained experimentally. The frequency versus acceleration curve was used to determine modal parameters i.e., natural frequency and damping factor.

The sample response of spindle was shown in Figure 3. The first three Natural frequencies of spindle are shown in table 1.

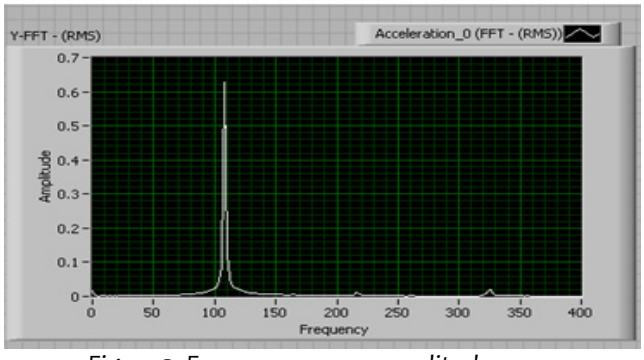

Figure 3. Frequency versus amplitude curve

Table 1. Modal Analysis of High motorized spindle (30,000 rpm) – First 2 Natural Frequencies

Measurement Location	Natural Frequencies(Hz)	
	Mode 1	Mode 2
Motorized High Speed Spindle	112	220

The mode shapes and damping factors of the structures were calculated using the results of the Fast Fourier Transform of the vibration signals from the accelerometer. By using the half-power band width method, we can find the damping factor of the spindle from the response curve frome equation 1.

$$\eta = (f2\text{-}f1)/fr$$

Where (f2-f1) and fr represent the half power band width and the corresponding natural frequency, respectively [9, 10, 11]. The damping ratio of the spindle is 0.060.

Numerical modal analysis of spindle

The modeling of spindle designs were done in ANSYS is shown in figure 4. The modal analysis was done using Subspace method to find first five natural frequencies and mode shapes [12].

The natural frequencies of form designs were tabulated for first 5 modes. First mode shape was axial mode. The second mode shape was bending mode shape, the third and fourth mode shapes were shear mode. The fifth was combined shear and bending mode.

Assumptions made to convert finite element dynamic model

- ☐ The spindle is treated as the space spring beam
- ☐ The angular contact ceramic ball bearing- radial compression spring mass unit
- ☐ The rotor, jacket and socket are axial material- additional distributing mass.

Element selection

Beam 188- spindle

- ☐ Nodes I,J

Degrees of freedom

- ☐ 3 translations
- ☐ 3 rotations

Special features

- ☐ The shearing effects are included by giving stiffness values in the section controls.

$$k_s = k_t * G * A$$

- ☐ It allows gyroscopic effects, includes in mode extraction damped and QR damped methods
- ☐ The coriolis is included by giving inertia force in terms of angular velocity.

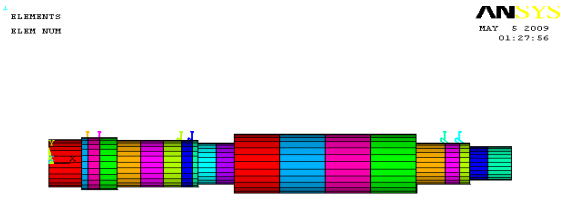

Figure 4. FEM modelof the High speed motorised high speed spindle

Combi -214 Bearing

- ☐ Nodes – I,J

Degrees of freedom

- ☐ 3D - radial spring
- ☐ K - spring constant

A. Stiffness of angular contact ball Bearing

$$K_{rs} = 1.25 * 10^{-7} * p^{0.33} * Z^{0.666} * \sin^{0.66}\alpha * \cos\alpha * D_b^{0.33}$$

$$K_r = K_{rs} * [1 - 1.92e - 10n^2] \text{ for } \alpha = 25^\circ$$

K_r – Radial stiffness when bearing is in static condition

K_{rs} – Radial stiffness when bearing is in dynamic condition

P – Preload, Z – No of balls. D_h – Diameter, α – Contact angle. n – Speed.

B. Section properties for Beam188 and real constants for Combi214

Section properties length, inner radius, outer radial, Area, add mass per unit length, and transverse shear stiffness are given as inputs. Radial stiffness of the bearing is calculated and given in the real constant. Stiffness of the bearing is function of initial preload and thermally induced preload. So it is necessary to estimate the thermally induced preload from the thermal analysis results

C. Thermally induced preload

Details for calculating thermally induced preload in table 2 and temperature difference are calculated for 5000 sec in table 3.

Table 2. Details for calculating thermally induced preload

Bearing set	Co efficient of thermal expansion of bearing steel =1.25*10e-5 /K				
	Xb (mm)	Dio (mm)	Doi (mm)	Db (mm)	Spring constant
I	23.92	127.4	104.18	9.525	9.402*10e9
II	21.89	110	91.3	8.731	10.239*10e9
III	30.16	100	82	7.938	10.639*10e9

Table 3. Temperature difference are calculated for 5000 sec

Bearing set	Temperature difference				
	inner race	outer race	bearing housing	shaft	ball
Front I	16.39	16.34	15.77	16.28	16.82
Front II	17.91	17.11	15.33	17.91	17.55
Rear	23.66	22.3	26.98	23.35	23.61

$$\Delta_1 = \alpha_s x_i \left(T_i^1 - T_i^o\right) - \alpha_s x_o \left(T_o^1 - T_o^o\right)$$

where αs is the linear expansion coefficient of steel which is the material of the shaft and sleeve; xi and xo are the distances of the contact points between the paired bearings of inner and outer rings; Ti1 and To1 are the new temperatures of the shaft and housing/spacer respectively.

The relationship of xi, xo and the distance of the centers of the bearing pair (xb) are

$$x_i = x_b + 0.5 D_b \sin\alpha$$

$$x_i = x_b - 0.5 D_b \sin\alpha$$

$$\Delta_b = 0.5\alpha_b D_b \left(T_b^1 - T_b^o\right)$$

$$\Delta_r = 0.5\alpha_s \left[D_{io}\left(T_{ir}^1 - T_{ir}^o\right) - D_{oi}\left(T_{or}^1 - T_{or}^o\right)\right]$$

where D_{io} is the inner diameter of the outer ring, D_{oi} is the outer diameter of inner ring, T_{ir}, is the temperature of the inner ring, and T_{or}, is the temperature of the outer ring.

$$\Delta = \Delta_1 + \Delta_r \cos\alpha - \Delta_a \sin\alpha$$

$$p_t = K_a \Delta^{1.5}$$

Initial preload and thermally induced preload is shown in table 4.

Table 4. Initial preload an thermally induced preload

Bearing set	Axial thermal deflection	Initial preload	Thermally induced preload	Total preload
I	8.90E-07	146	7.59	153.59
II	1.14E-06	123	12.42	135.42
III	2.15E-06	50	33.53	83.53

The stiffness of the bearing is greatly affects natural frequencies. Actually, it increases the natural frequencies. The thermally induced preload is estimated for 10000rpm speed.

D. Modal analysis

Table 5 the natural frequencies including centrifugal and gyroscopic effects of spindle bearing system without including thermally induced preload.

Table 5. Natural frequencies including centrifugal and gyroscopic effects of spindle

Speed	Natural frequencies (Hz)					
	Mode I		Mode II		Mode III	
Effects	Centrifugal	Gyroscopic Forward	Centrifugal	Gyroscopic Forward	Centrifugal	Gyroscopic Forward
		Backward		Backward		Backward
10000	122	122.67	224	225.392	625	632.02
		121.71		222.43		619.80
50000	89.4	91.781	163	172.86	613	645.24
		86.763		155.58		583.24

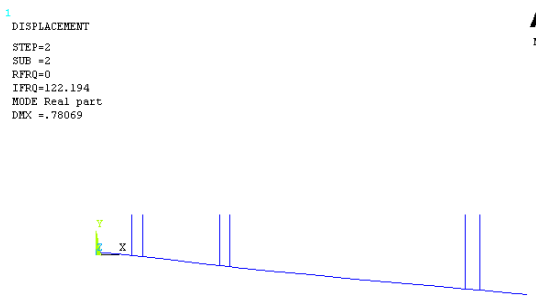

Figure 5 a. I mode shape for 122 Hz

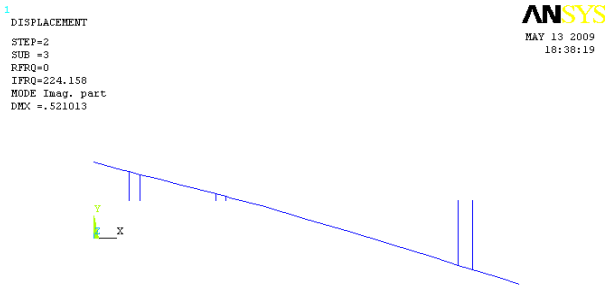

Figure 5 b. II mode shape for 224 Hz

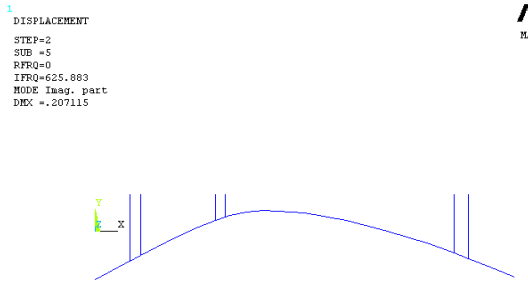

Figure 5 c . III mode shape for 625Hz

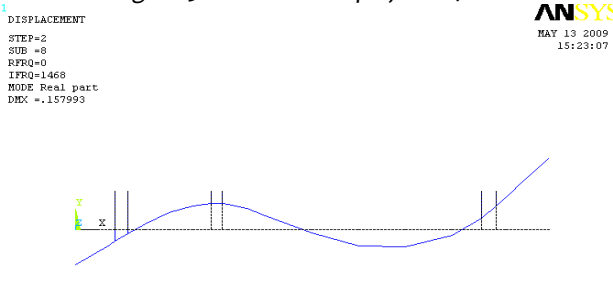

Figure 5 d. IV e mode shape for 1428Hz

Figure 5. Mode shape of High motorized spindle

The model has been created using beam 188 and combi214. The sections are created to give dimensional properties for beam188 and stiffness is given to combi214. The coriolis is included by giving inertia force in terms of angular velocity to include the effect of centrifugal effects. Gyroscopic effect included by extracting by QR damped method Campbell diagram shows the extracted damped frequencies.

RESULTS AND DISCUSSION

A. Thermally induced preload on natural frequencies

The thermally induced preload has been estimated from the thermal analysis for 10000 rpm. The thermally induced preload and corresponding stiffness has also been calculated and tabulated. The natural frequencies including initial preload, thermally induced preload, centrifugal and gyroscopic effects have been extracted and tabulated. The critical speeds have also been calculated.

Table 6. The critical speed by including all the effects.

Speed	Natural frequencies (Hz)					
	Mode I		Mode II		Mode III	
Effects	Centrifugal	Gyroscopic Forward	Centrifugal	Gyroscopic Forward	Centrifugal	Gyroscopic Forward
		Backward		Backward		Backward
10000	131	132.15	228	229.392	627.6	633.02
		131.3		226.43		621.58
Critical speed	7870		13573		37294	

These values is given in the table 5 The natural frequencies are extracted with and without these effects have been studied and found that the important of each effects .The critical speed is not uniform in any of the modes because the preload is varying depends on the time .so the time increases the natural frequencies increases. It seems to be good effect as increases the operating range. But the excess of thermally induced preload will cause the bearing failure. So the material should have more thermal stability to withstand The thermally al stability to withstand temperature. If the material gets thermal deflection after a long time of operation, the thermally induced preload will be good to lift up the critical speed to have higher speed without bearing failure.

Table 7. Modal analysis Comparison of spindle

S.No	Natural Frequencies(Hz)			
Motorized High Speed Spindle	Experimental		Numerical	
	Mode-I	Mode- II	Mode-I	Mode- II
	112	220	122	224

B. The critical speed by including all the effects

The critical speed has been calculated from the Campbell diagram which is available in ANSYS. The results has been given, are for 10000 rpm speed and 5000 seconds .

CONCLUSIONS

The natural frequencies are extracted by considering stiffness and mass of the body will not be sufficient to find critical speed for high speed spindle. Because the stiffness of the rotating body will be varying depends on the speed. So the speed effects like centrifugal and gyroscopic effects of the spindle bearing system have been considered. The centrifugal and the gyroscopic effects are damping the natural frequencies significantly.

The gyroscopic effects are damping the natural frequencies little than the centrifugal effects and these effects can be minimized by keeping same shaft cross-section and placing motor in the middle position to have mass balance.

The centrifugal effects can be reduced if the cross sections are reduced but the strength of the spindle depends on the cross section so these effects cannot be minimized effectively so the preload should be increased to balance the damping to have higher critical speed. The stiffness of the bearing based on preload which is given by locknut only will not be sufficient. The thermally induced preload should also be included to have more and appropriate preload because if you give only initial preload to compensate the centrifugal and gyroscopic damping, the thermally induced preload will be added due to thermal behavior and will cause bearing failure.

The preload which is given by both thermally induced and through locknut is shared to lift up the critical speed to have higher range of operating speed. The estimation of thermally induced preload and corresponding natural frequencies has been calculated and shown that critical speed has been lifted to have high range of operating speed for 10000 rpm for different time .

REFERENCES

[1.] C.Salomon, 1931 ,Verfahren zur Bearbeitung von Metallen oder Bei Bearbeitung durch schneidende Werkzeuge von sichah nlich Verhaltenden Werkstoffen, Deutsches Patent Nr.523594,April.

[2.] R.Komanduri, J.McGee, R.A.Thompson ,J.P.Covy, F.J.Trun-cale, V.A.Tipnis, R.M.Stach, R.I.King, On a methodology for establishing the machine tool system requirements for high-speed/high-through put machining, Journal of Engineering for Industry,TransactionsoftheASME107(1985)316–324.
[3.] M.Kaufeld, High-speed milling from a user's and machine builder's viewpoint, Werkstatt and Betrieb 123 (10) (1990) 797–801.
[4.] B.Bossmanns ,J.F.Tu,T hermalmodel for high speed motorized spindles, International Journal of Machine Tools and Manufacture,39(9)(1999)1345-1366.
[5.] B.Bossmanns,J.F.Tu, A power flow model for high speed motorized spindles—heat generation characterization, ASME Journal of Manufacturing Science and Engineering 123(3)(2001) 494–505.
[6.] Heisel, M Gringel, "Machine Tool Design Requirements for High Speed Machining", in CIRP Annals-Manufacturing Technology, volume 45, Issue 1, (1996), Pages 389-392.
[7.] Bernd Bossmanns, Jay F. Tu, August 2001. "A Power Flow Model for High Speed Motorized Spindles-Heat Generation Characterization". Transactions of the ASME Vol-123.
[8.] Mohammad R. Movahhedy, Peiman Mosaddegh 21 September 2005 "Prediction of chatter in high speed milling including gyroscopic effects". International Journal of Machine Tools & Manufacture 46 (2006) 996–1001
[9.] Jung Do Suh and Dai Gil Lee, "Design and manufacture of hybrid polymer concrete bed for high-speed CNC milling machine", International journal of Mechanical Material Design, volume 4, (2008), Pages 113-121.
[10.] Ju Ho Kim, Jae Eung Lee, and Seung Hwan Chang, " Robust design of microfactory elements with high stiffness and high damping characteristics using foam-composites and sandwich structures", in Composite Structures, volume 86, (2008), pages 220-226.
[11.] Dai Gil Lee, Jung Do Suh, Hak Sung Kim, and Jong Min Kim, "Design and manufacture of composite high speed machine tool structures", in Composites Science and Technology", volume64, (2004), pages 1523-1530.
[12.] Michael R Hatch, Vibration Simulation using ANSYS and Matlab.

ANNALS OF FACULTY ENGINEERING HUNEDOARA
– INTERNATIONAL JOURNAL OF ENGINEERING